https://doi.org/10.33271/nvngu/2022-3/017

F. Baladah[1],
orcid.org/0000-0002-3491-253X,
M. Chettibi[1],
orcid.org/0000-0002-2794-7937,
A. Boutrid[2,3],
orcid.org/0000-0002-1041-3904,
A. Bouhedja[1],
orcid.org/0000-0002-4289-8272

1 – Faculty of Earth Science, Mining Department , University of Badji Mokhtar-Annaba, Algeria, e-mail: fbaladah2@gmail.com
2 – Laboratory of Mineral Processing and Environment, University of Badji Mokhtar-Annaba, Algeria
3 – Department of Civil Engineering, Abbèss Laghrour University, Khenchela, Algeria

MINERALOGICAL AND GRANULO-CHEMICAL CHARACTERIZATION OF VEINS 4 AND 10, OF AIN MIMOUN BARYTE ORE MINE

Purpose. The purpose of the carried out granulo-chemical and mineralogical study, realised on barite of two veins 4 and 10 of Ain Mimoun deposit (Algeria), is the identification of the barite ore in order to be able to choose a reliable processing method due to its complicated structure.

Methodology. The investigation was carried out by X-Ray Diffractions (XRD), Scanning Electron Microscope (SEM), X-Ray Fluorescence (XRF), particle size analysis and microscopic observations.

Findings. Using the investigation devices, predominance of barite minerals was found at 51 %, quartz in the vicinity of 34 % and calcite at 9 %, with a homogeneous distribution in all the fractions observed. Adding to that, the main compounds (oxides) present are SiO_2, CaO, Fe_2O_3, Al_2O_3, P_2O_5, Na_2O, K_2O, TiO_2, and MnO.

Originality. For the first time the characterization of veins 4 and 10, in which the barite particles are embedded in silica, has been realised for the purpose of proving the possibility of their processing.

Practical value. The obtained results confirm, on the one hand, that veins 4 and 10 are rich in barite and, on the other hand, barite particle release from silica particles is possible. Thus, we suggest, for a better and diversified use of the ore of the veins in question, the application of the flotation process, since the latter makes it possible to obtain high-quality concentrates, so it can be used not only in the petroleum field but also in the pharmaceutical and other industries.

Keywords: *Ain Mimoun Mine, barite ore, vein 4 and 10, enrichment, Algeria*

Introduction. Barium sulphate, which is commonly known as Barite, is one of the most important industrial minerals and extensively used in many areas such as oil drilling, hydraulics, catalyst carriers [1, 2], adsorbent materials [3, 4], as well as in the chemical (painting) and radioscopic industries [5]. Among others, it can be used as a gas sensor for vacuum tubes, lubricant (additive) and in filler and dye for paper [6–8]. Regarding all this wide use presenting this mineral, the demand for barite increases exponentially. To this end, the mining industry in Algeria deals with the exploitation of this type of ore.

On a national scale it excites a significant number of barite deposits, namely, Boucaid W. Tissemsilt; Mellal W. of Tlemsen; Koudiat Safa W. of Medea; Djbel Draissa W. of Bechar, and the largest and most important deposit is of Ain Mimoun. The barite deposit of Ain Mimoun is located on the territory of the wilaya of Khanchela, 28 km west of the capital. It was discovered in 1968 during the geological work on revision of the region of the anticline of Khenchela by the base (B) of the former SONAREM. The special research work following the barite veins with evaluation of the reserves was carried out from 1968 to 1970.

The Barite of Ain Mimoun is linked to an epigenetic mineralogical procession of hydrothermal type. Barium sulphates can be deposited in a sedimentary environment under the effect of hydrothermal solutions and several mechanisms such as digenetic processes. Barite can be formed under the effect of direct precipitation when a barium-rich hydrothermal fluid reacts with mineralizing solutions constrained to an environment of diapiric masses; like that of the Khenchela region. The origin of these mineralizing solutions is probably only the brines from the sub-side sedimentary basins, during a compressive tectonic phase, where hot and salty fluids are expelled and then diluted by others less hot and less salty (surface waters).

Ain Mimoun deposit is extending on the northern flank of the anticlinal of Khenchela, on a total area of 614 hectares. The deposit is located about 10 kilometres North of Tamza town, 8 km of the South-West of the Daira of El Hamma and about 16 km to the West of Khenchela city, where it is related administratively. The geographic location is illustrated in Fig. 1. [5].

The extent of the barite veins in the direction varies widely from (20–50) to 1,400 m; depending on how the extent stands out, the large veins are more than 400 m in length, (N° = = 01.02.03.04.05.10 and 11); medium veins from 100 to 400 m, from (No. 5.06.07.08.09.12) and small veins from first tens of meters to 100 m, in depth the veins are up to 50–100 m.

In our work, we are interested in the two veins, vein 4, which is located 11 km southeast of the treatment plant, whose SiO_2 content is 10.04 %. The tenth vein is located 15 km southeast of the treatment plant with a silica content (SiO_2) that varies between 2.86 and 53.41 %, on average of 16 %.

At present, the processing of barite ore of veins 10 and 4 poses certain difficulties because of its mineralogical structure. Mineralogical analysis has shown that the barite particles are encrusted with those of silica, which makes their separation difficult by jigging at the Ain Mimoun plant.

Therefore, the objective of this work is to carry out a broad granulo-chemical and mineralogical characterization of the representative samples taken from the two veins 4 and 10, by means of sieving analysis, X-ray Diffraction (DRX), microscopic observation of different particle size slices under a binocular microscope; X-ray fluorescence (FRX) as well as scanning electron microscopy (SEM-EDX), in order to identify veins 4 and 10, and to be able to choose a reliable process for enriching the ore of the latter.

Materials and methods. ***Sampling.*** Sampling is a crucial step in the characterization process. The aim is to obtain a representative range of samples that reflect all the physical and chemical characteristics of the entire studied site.

The sample used for our study was taken and stored by the laboratory engineer of the processing unit whose weight is 800 g. For security measures it was not possible to carry out sampling individually.

Granulometric analysis. For particle size analysis the sieving method is used. These fractions are made up of particles whose size covers a relatively small interval and decreases from

© Baladah F., Chettibi M., Boutrid A., Bouhedja A., 2022

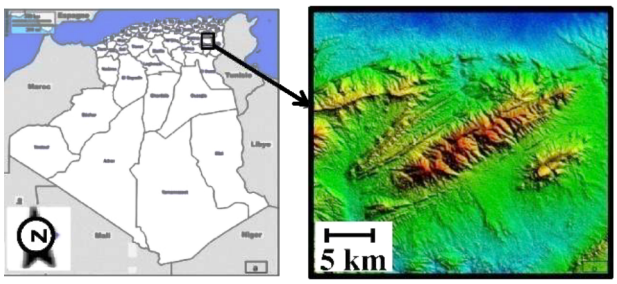

Fig. 1. Geographical location of the studied area:

a – geographic map of Algeria; b – DTM digital terrain model of the area of the studied mines [9]

one fraction to another. The series of sieves used are of the following meshes: (4; 2; 1; 0.5; 0.25; 0.125; 0.063; 0.045) mm. The previously heavy dried sample of 800 grams is introduced on the top sieve and the entire battery is subjected to a horizontal and vertical shaking movement thanks to a sieving device (electric sieve), for 20 min. The results of the sieving are compiled in three steps:

1. Calculation of the mass percentage of each fraction.
2. Calculation of the cumulative percentage retained on each sieve.
3. Calculation of the cumulative percentage passing from each sieve.

***X-ray diffraction* (*XRD*).** X-ray diffraction is a non-destructive analysis technique that allows us to know the structure and crystallographic phase of all samples; thus, crystallite sizes have been identified. The principle of the method is based on the diffraction of X-rays by a family of reticular planes (hkl) favourably oriented at an angle θ with respect to the incident beam. These parameters are connected by Bragg's law

$$n\lambda = 2d \sin\theta.$$

The X-ray diffraction (XRD) diagrams were obtained using a Bruker D8 Advance Diffractometer with Cu Ka radiation of λ = 1.5406 Å, with Nickel (Ni) filter in the 2θ scan range from 15 to 60°, with data collection every 0.05° and with a downtime in each angle of one second.

***Scanning Electron Microscopy* (*SEM-EDX*).** The SEM technique combined with EDX is a technique for observing the topography at the microscopic scale and the chemical composition of surfaces; it makes it possible to give images on the surface of a high-resolution sample and the possible dispersion of particles on the surface. The principle of this technique is based on electron-matter interactions; it consists in scanning the surface of a sample with an electron beam and analysing the secondary or backscattered reflected electrons that come from the surface layer of samples. The analyses were carried out on eight particle size units of the barite ore using a SEM scanning electron microscope at the laboratory of the National School of Mining and Metallurgy in Annaba. They consisted of imaging using an FTI QUANTA 250 microscope. In addition, this is in order to study the morphology of the main minerals that make up the barite ore and their chemical composition on the surface.

Sample preparation. The sample used for our study was taken and stored by the laboratory engineer of the processing unit. For safety measures it was not possible to carry out sampling individually; study therefore allows the orientation of the choice of the enrichment technique to be adapted. The different analyses involved in the characterization frequently require sample preparation. The preparation procedure involves several operations, which must therefore be carried out in such a way as to preserve the integrity of the samples. Dry grinding lasts for 10 min, until a size class –8 +20 mm is obtained. Homogenization and quart are essential operations for the reduction of the weight and volume of the sample and the obtaining of two main samples, one intended for characterization and the other as a control sample. The weight of the sample intended for characterization is 800 g.

Results and interpretations. ***Particle size analysis and microscopic observation*.** The results of the particle size analysis are presented in Table 1, and illustrated in Figures. From the results obtained, it is noted that the large part of the overall mass of the sample is included in the range (–500 + 125) μm, it is of the order of 208.17 g with a weight yield of 26.02 %. On the other hand, the coarse slice yield greater than 4 mm is 1.07 %. The fine fraction less than 63 μm represents only 13.65 % (Table 1).

The results of the sieving analysis of the phosphate ore of Jebel Onk veins 4 and 10 presented in Table 1 and illustrated in Fig. 2, show that the cumulative yields of passing particles are increasing according to the meshes of the sieves. On the one hand, the cumulative returns of the retainers are decreasing according to the openings of the sieves. On the other hand, we note that the two curves (passing and retaining particles) are symmetrical and intersect at point D50. The curve of the results of the particle size analysis of the cumulative yields of the refusals is of a concave shape, which means the predominance of large particles compared to *Observation under a binocular microscope.*

The size classes for microscopic observation are (–0.5 +0.25); (–0.25 +0.125) and (–0.125 +0.063), the latter were previously washed and dried in the oven at 60 °C until a constant weight was obtained. The observation was carried out under a binocular microscope of the laboratory of the Geology

Table 1

Results of particle size analysis of a representative sample of veins 4 and 10

Granulometric Fractions, mm	Yield Weight, g	Yield Partial, %	Yield Cumulative refusal, %	Yield Cumulative Passing, %
+4	1.07	0.13	**0.13**	**100**
–4 +2	14.21	1.78	**1.91**	**99.87**
–2 +1	56.21	7.03	**8.94**	**98.09**
–1 +0.5	153.89	19.24	**28.18**	**91.06**
–0.5 +0.25	208.17	26.02	**54.2**	**71.82**
–0.25 +0.125	153.26	19.16	**73.36**	**45.8**
–0.125 +0.063	103.91	12.99	**86.35**	**26.64**
–0.063 +0.045	83.45	10.43	**96.78**	**13.65**
–0.045 +0	25.83	3.22	**100**	**3.22**
Total masse	**800**			

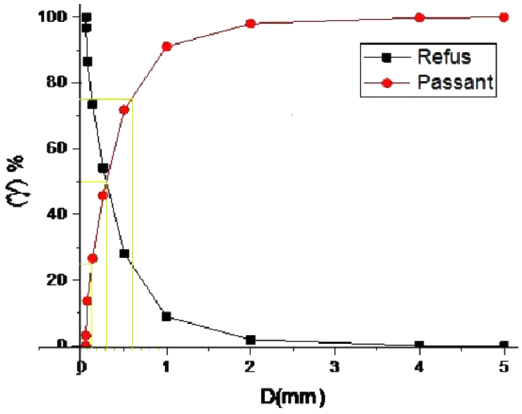

Fig. 2. Granulometric curves

Department of Annaba University, the microscopic observation results are illustrated in Fig. 3. The results of the mineralogical analysis by counting are presented in Table 2.

From the obtained results, it is clear that in all figures, barite particles are well freed from those of silica and quartz, which gives an ease of separating them from the gangue in which they are embedded. The analysis by microscopic counting shows the predominance of barite minerals at 51 %, quartz in the vicinity of 34 % and ultimately calcite at 09 %, with a homogeneous distribution in all fractions observed.

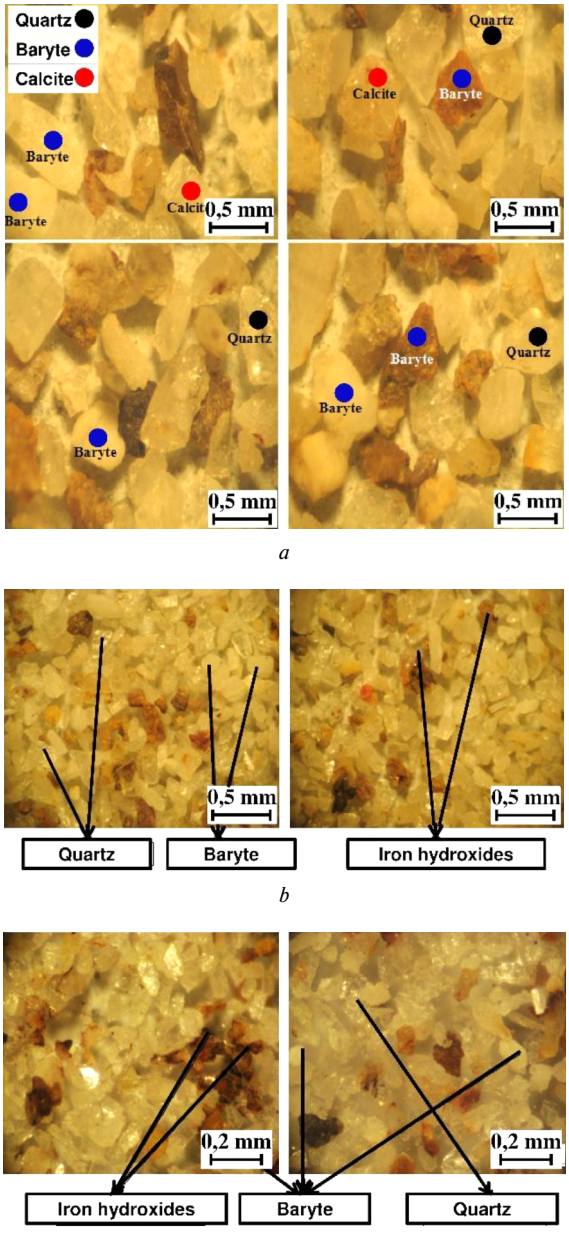

Fig. 3. Observation results of the different fractions under the binocular microscope:

a – (–0. 5 +0.25 *mm*); *b* – (–0.25 +0.125 *mm*); *c* – (–0.125 +0.063 *mm*)

Table 2

Results of mineralogical analysis by microscopic counting

Particle size class, mm	Barite, %	Calcite, %	Quartz, %	iron hydroxide, %	Other, %
–500 +20	50.07	8.87	33.76	1.77	5.53
250 + 125	52.87	9.55	33.24	1.72	2.62
–125 + 63	50.60	8.59	35.57	2.1	3.14

Analysis by DRX. The X-ray diffraction patterns of barium sulphate particles for different states (micrometric powder, nanometric powder, micrometric powder calcined at 1000 °C, and micrometric powder calcined at 1200 °C) are shown in Fig. 4. The X-ray diffraction study was used to identify the crystal structure and determine the particle size. All the reflection plains are matched with an orthorhombic phase of barium sulphate [10–12], with crystalline cell constants a = 7.144, b = 8.865 and c = 5.445A°, which are basically in agreement with the reported values (JCPDS Card Files No. 80-0512), space group Pnma.

The crystalline sizes of the natural barite are calculated using Scherer's formula [13] for the four high intensity peaks observed at 22.84, 24.93, 31.60, 32.84, 42.61, and 42.99°(2θ) with hkl values (111), (200), (211), (002), (140), and (410), an example of a peak is shown in Fig. 5. With λ the X-ray wavelength (0.15406 nm) and θ the Bragg diffraction angle. The values of β and θ parameters are estimated by Gaussian fitting of the XRD peaks. This formula is not limited by the preferential orientation and is valid for an ordinary XRD profile. The differences in the widths of the peaks indicate differences in crystallite sizes and also specific surfaces. Scherrer's method makes it possible to estimate the average size of crystallites, when they are less than 100 nm. Scherrer's formula is written

$$D = \frac{K \cdot \lambda}{\beta hkl \cdot \cos(\theta hkl)}; \quad (1)$$

$$\beta hkl = W \frac{\pi}{180}; \quad (2)$$

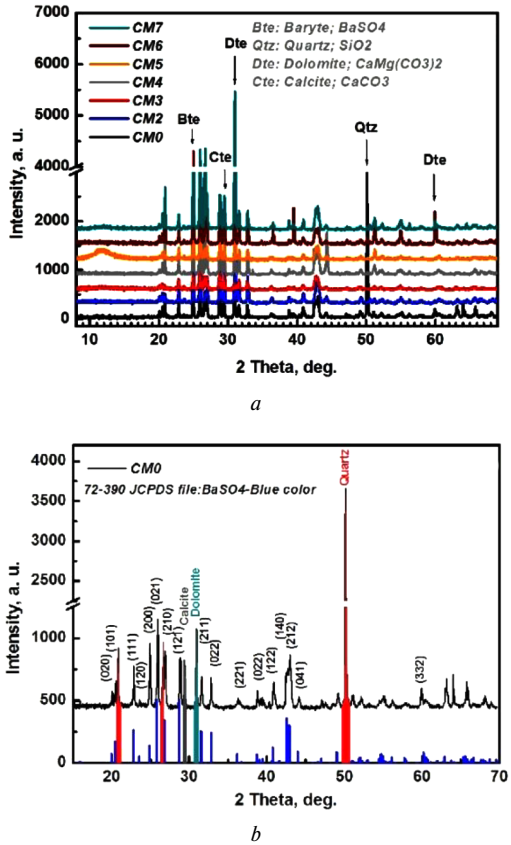

Fig. 4. Results of X-ray diffraction pattern of different particles size fractions:

a – 0 ≤ *Intensity*, *a.u* ≤ 5500; *b* – 0 ≤ *Intensity*, *a.u* ≤ 1500

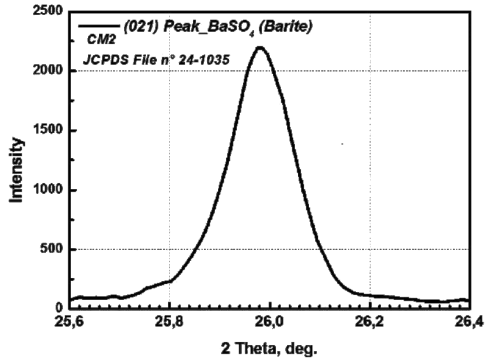

a

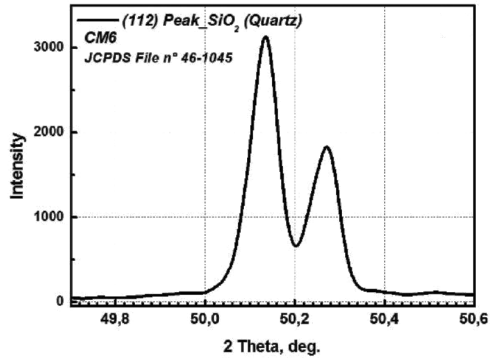

b

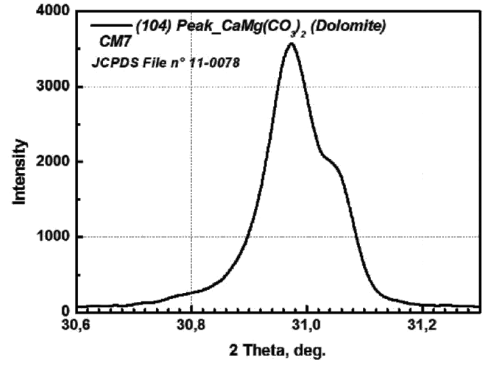

c

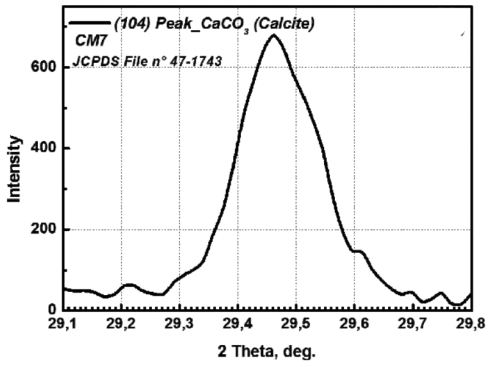

d

Fig. 5. RX diffraction peaks representative of the various phases present in the barite:

a – Barite; b – Quartz; c – Dolomite; d – Calcite

$$Sa = \frac{6}{\rho \cdot D}, \qquad (3)$$

where D is the average size of crystallites in the direction perpendicular to the planes (hkl); K is the constant; λ is the monochromatic wavelength, in our case it corresponds to the doublet CuKα1 + α2; βhkl is the full width half maximum (FWHM) of X-ray diffraction peak in radians; $2\theta hkl$ is Bragg angle at the top of the chosen line; ρ is the density of the oxide; Sa is the specific surface of the oxide.

The results of calculations are shown in Figs. 6, *a, b*, which correspond to the values of the size crystallites, as well as specific surfaces. The average crystallite size of barite is estimated to be around ~43 nm. The specific area inversely proportional to D, it is of the order of ~ 33 m^2/g, in accordance with the data of the literature [14].

X-ray fluorescence analysis "FRX". X-ray fluorescence spectrometry (XRF) is an X-ray instrumentation used for chemical analyses, relatively non-destructive, it allows analysing the main compounds and also the constituent traces of rocks, minerals, sediments and fluids. The analysis of major elements and traces in geological materials by XRF is feasible by the responses-interaction of atoms when they interact with X-rays [15, 16].

The results of XRF analysis recapitulated in Tables 3 and 4, confirms the presence of the various components of barite, in this case we can draw Table 3, giving the mass percentages of $BaSO_4$, SiO_2, CaO, Fe_2O_3, Al_2O_3, P_2O_5, K_2O, Na_2O, TiO_2, MnO, and other oxides such as ZnO, CuO, etc.

Fig. 7 below shows the main compounds (oxides) present in addition to barite, among which we cotton in order of presence: SiO_2, CaO, Fe_2O_3, Al_2O_3, P_2O_5, Na_2O, K_2O, TiO_2, MnO, and PAF (loss to fire)/L.O.I. is loss on ignition; which corresponds to the elements that evaporated during the analysis (organic and other inorganic elements).

Morphological analysis by SEM and EDX. The micrographs of the various powders are shown in Fig. 8. There are grains of whitish colour, corresponding to the barite, and rather grey grains that can be associated with dolomite or calcite.

Barite mineral is soft but heavy, slightly tinged with white, grey, yellow or brownish. Barite is a mineral species composed of

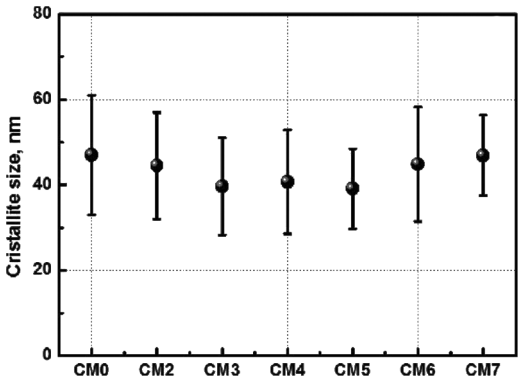

a

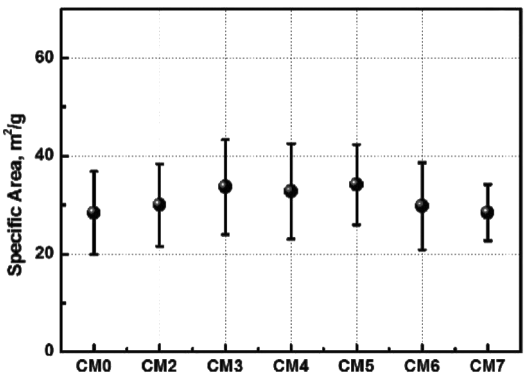

b

Fig. 6. Results of calculation of:

a – Crystallite size values; b – Specific barite surfaces

Table 3

X-ray fluorescence analysis results

	Fluorescence X analysis, %											
	SiO_2	**Al_2O_3**	**Fe_2O_3**	**CaO**	**MgO**	**Na_2O**	**K_2O**	**TiO_2**	**MnO**	**P_2O_5**	**PAF**	**$BaSO_4$**
CM0	13.06	1.38	2.94	7.79	< 0.05	< 0.05	< 0.05	< 0.05	< 0.05	0.32	6.08	67
CM2	11.83	1.10	3.28	11.13	< 0.05	< 0.05	< 0.05	< 0.05	< 0.05	0.29	11.30	57.64
CM3	10.94	1.61	2.12	6.68	< 0.05	< 0.05	< 0.05	< 0.05	< 0.05	0.48	8.92	73.51
CM4	13.38	1.42	2.59	7.65	< 0.05	< 0.05	< 0.05	< 0.05	< 0.05	0.44	5.97	66.29
CM5	13.68	1.28	2.55	7.98	< 0.05	< 0.05	< 0.05	< 0.05	< 0.05	0.58	8.04	65.57
CM6	15.02	2.14	3.86	9.21	< 0.05	< 0.05	< 0.05	< 0.05	< 0.05	0.68	8.58	57.70
CM7	14.29	2.27	4.02	9.47	< 0.05	< 0.05	< 0.05	< 0.05	< 0.05	0.76	7.40	60.56

Table 4

Average concentrations of different chemical components of the samples

	Fluorescence X analysis, %											
	SiO_2	**Al_2O_3**	**Fe_2O_3**	**CaO**	**MgO**	**Na_2O**	**K_2O**	**TiO_2**	**MnO**	**P_2O_5**	**PAF**	**$BaSO_4$**
Average	13.23 +/– 1.29	1.56 +/– 0.41	3.12 +/– 0.56	8.68 +/– 1.37	< 0.05	< 0.05	< 0.05	< 0.05	< 0.05	0.53 +/– 0.16	11.72 +/– 4.05	64.26 +/– 5.33

barium sulphate $BaSO_4$ formula with traces of Sr, Ca and Pb. On hydrothermal origin, barite presents various compositions. Rich in Pb, Sr, C, Ra, or several of these elements associated with them or other, dedicate this mineral to the multiple uses. This mineral usually crystallizes as flattened crystals, sometimes lamellar. Crystals are tubular, prismatic, and as grainy, platy, and coxcomb aggregates. Crystals may be present in aggregates (typically cleavable), and these crystals are lenticular grouped into rosettes. Individual crystals are often twinned, and can be quite large. May also be massive, nodular, fibrous, stalactitic, and as perfect rosettes. Macro-graphic images are shown in Fig. 8.

The results of EDX analyses (Fig. 9) confirm the presence of the elements Ba, S, O, Si, Ca, Mr, Fe, Al, corresponding to the presence of the compounds Barite, Quarters, Dolomite, calcite, iron oxide, aluminium oxide.

Conclusions. The experimental obtained results allowed us to conclude the following:

1. Particle size analysis and microscopic observation of different particle size slices testify to the good release of barite from the gangue in the following fractions: (–0.5 +0.25); (–0.25 +0.125) and (–0.125 +0.063).

2. The predominance of barite minerals at 51 %, quartz in the vicinity of 34 % and at the end calcite at 0.9 %, with a homogeneous distribution in all the fractions is observed; these results correspond to the results of DRX.

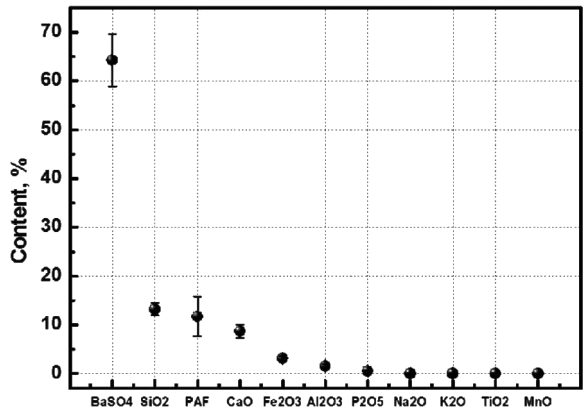

Fig. 7. Main compounds (oxides) present in addition to barite

3. The micrographs of the various powders mention whitish grains, corresponding to barite, and rather grey grains that can be associated with dolomite or calcite.

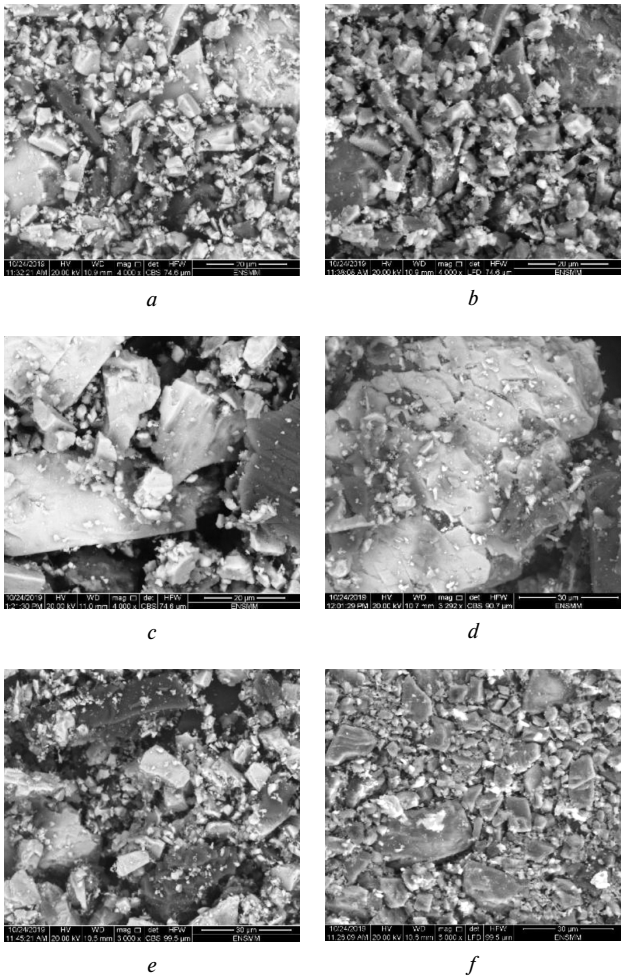

a *b* *c* *d* *e* *f*

Fig. 8. Results of SEM of:

a – CM3 P3-039; b – CM3 P3-048; c – CM7 P7-072-045; d – CM5 P5-072-012; e – CM4 P4-058; f – M4 P4-064

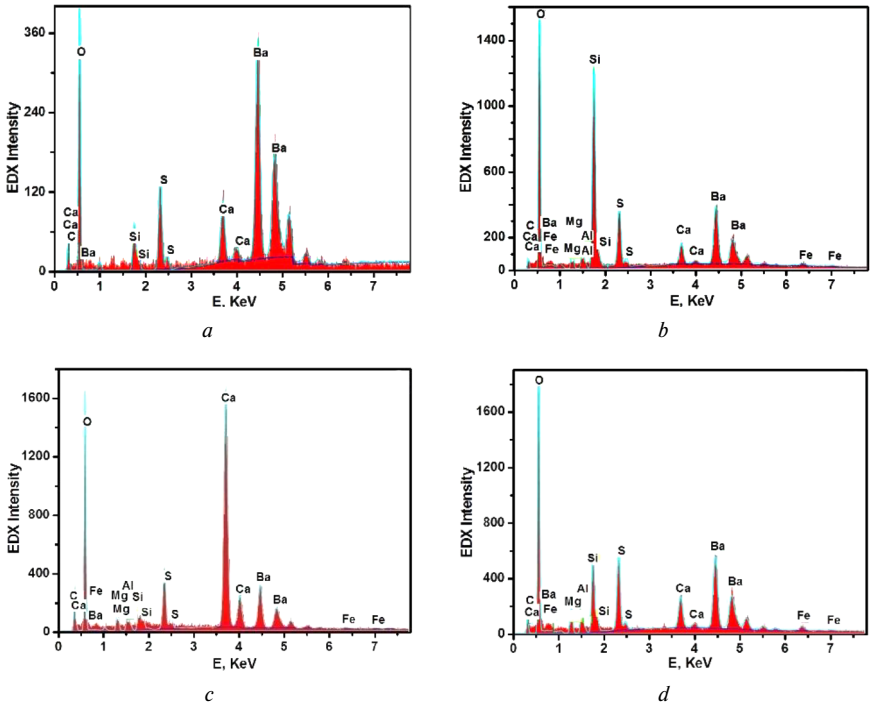

Fig. 9. Combined results of EDX analysis of:
a – CM3; b – CM4; c – CM5; d – CM7

4. The presence of the elements Ba, S, O, Si, Ca, Mr, Fe, Al, corresponding to the presence of the compounds Barite, Quarters, Dolomite, calcite, iron oxide, aluminium oxide, proven by FRX and EDX.

Following the results of the mineralogical and granulochemical characterization carried out on the representative sample of veins 4 and 10, the separation of Barium sulphate $BaSO_4$ embedded in silica is possible by grinding to a particle size of less than 500 µm or a very good release of barite is ensured. We suggest, for a better and diversified use of the ore of the veins in question, the application of the flotation process [17, 18], since the latter makes it possible to obtain high-quality concentrates, so it can be used not only in the petroleum field but also in the pharmaceutical and other industries.

Acknowledgments. *The authors express their sincere gratitude to Laboratory managers and engineers of "LAVAMINE", Mining Department, Badji Mokhtar Annaba University, and Higher School of Mining and Metallurgy Annaba, Algeria, for their help in carrying out this scientific research.*

References.

1. Ghashang, M. (2012). Preparation and Application of Barium Sulfate Nano-particles in the Synthesis of 2,4,5-Triaryl and N-Aryl(Alkyl)-2,4,5-Triaryl Imidazoles. *Current Organic Synthesis, 9*(5), 727-732. https://doi.org/10.2174/157017912803251800.

2. Li, F., & Yuan, G. (2005). Low temperature catalytic conversion of methane to methanol by barium sulfate nanotubes supporting sulfates: $Pt(SO_4)_2$, $HgSO_4$, $Ce(SO_4)_2$ and $Pb(SO_4)_2$. *Chemical Communications*, (17), 2238. https://doi.org/10.1039/b500147a.

3. Lin, J., & Gao, H.-W. (2009). SDBS@$BaSO_4$: an efficient wastewater-sorbing material. *Journal of Materials Chemistry, 19*(22), 3598. https://doi.org/10.1039/b904303a.

4. Romero-Ibarra, I.C., Rodríguez-Gattorno, G., García-Sánchez, M.F., Sánchez-Solís, A., & Manero, O. (2010). Hierarchically Nanostructured Barium Sulfate Fibers. *Langmuir, 26*(10), 6954-6959. https://doi.org/10.1021/la904197k.

5. Wu, J., Barbero, R., Vajjhala, S., & O'Connor, S.D. (2006). Real-Time Analysis of Enzyme Kinetics via Micro Parallel Liquid Chromatography. *ASSAY and Drug Development Technologies, 4*(6), 653-660. https://doi.org/10.1089/adt.2006.4.653.

6. Hall, G.S., & Chambliss, C.R. (2004). Nondestructive Multi-Elemental Analyses of Current-Size United States Federal Reserve Notes by Energy Dispersive X-Ray Fluorescence. *Applied Spectroscopy, 58*(11), 1334-1340. https://doi.org/10.1366/0003702042475466.

7. Qu, M.-H., Wang, Y.-Z., Wang, C., Ge, X.-G., Wang, D.-Y., & Zhou, Q. (2005). A novel method for preparing poly(ethylene terephthalate)/BaSO4 nanocomposites. *European Polymer Journal, 41*(11), 2569-2574. https://doi.org/10.1016/j.eurpolymj.2005.05.

8. Yao, C., & Yang, G. (2009). Synthesis, thermal, and rheological properties of poly(trimethylene terephthalate)/$BaSO_4$ nanocomposites. *Polymers for Advanced Technologies, 20*(10), 768-774. https://doi.org/10.1002/pat.1313.

9. Batouche, T., Bouzenzana, A., Zedam, R., & Bourourou, M. (2019). Mineralogical and physico-chemical characterization of barite wastes fromAin Mimoun deposit (Khenchela, Algeria). *Solid State Physics, Mineral Processing,* 29-35. https://doi.org/10.29202/nvn-gu/2019-3/5.

10. Manam, J., & Das, S. (2009). Thermally stimulated luminescence studies of undoped, Cu and Mn doped $BaSO_4$ compounds. *Radiation Effects and Defects in Solids*, *163*(12), 955-965. https://doi.org/10.1080/10420150802163869.

11. Sivakumar, S., Soundhirarajan, P., Venkatesan, A., & Khatiwada, C.P. (2015). Spectroscopic studies and antibacterial activities of pure and various levels of Cu-doped $BaSO_4$ nanoparticles. *Spectrochimica Acta Part A: Molecular and Biomolecular Spectroscopy, 151*, 895-907. https://doi:10.1016/j.saa.2015.07.048.

12. Lane, M.D. (2007). Mid-infrared emission spectroscopy of sulfate and sulfate-bearing minerals. *American Mineralogist, 92*, 1-18. https://doi.org/10.2138/am.2007.2170.

13. Hargreaves, J.S.J. (2016). Some considerations related to the use of the Scherrer equation in powder X-ray diffraction as applied to heterogeneous catalysts. *Catalysis, Structure & Reactivity, 2*(1-4), 33-37. https://doi.org/10.1080/2055074X.2016.1252548.

14. Singaravelan, R., & Bangaru Sudarsan Alwar, S. (2014). Effect of reaction parameters in synthesis. Characterisation of electrodeposited zinc nanohexagons. *Journal of Nanostructure in Chemistry, 4*(4), 109-117. https://doi.org/10.1007/s40097-014-0121-2.

15. Temitope, D., & Timothy, O. (2018). X-ray fluorescence (XRF) in the investigation of the composition of earth materials: a review and an overview. *Geology, Ecology, and Landscapes, 2*(2), 148-154. https://doi.org/10.1080/24749508.2018.1452459.

16. Al-Eshaikh, M.A., & Kadachi, A. (2011). Elemental analysis of steel products using X-ray fluorescence (XRF) technique. *Journal of King Saud University – Engineering Sciences, 23*(2), 75-79. https://doi.org/10.1016/j.jksues.2011.03.002.

17. Chettibi, M., & Abramov, A.A. (2016). Development of Sphalerite activation regularity by copper Sulphate. *Journal of Mining Science,*

52(05). ISSN: 1062-8736. Edition Springer. https://doi.org/10.1134/S1062739116041526.
18. Nettour, D., Chettibi, M., Bouhadja, A., & Bulut, G. (2018). Determination of physicochemical parameters of Djebel Onk phosphate flotation (Algeria). *Naukovyi Visnyk Natsionalnoho Hirnychoho Universytetu*, (4), 43-49. https://doi.org/10.29202/nvngu/2018-4/8.

Мінералогічна та грануло-хімічна характеристика жил № 4 і 10 баритової шахти Айн Мімун

Ф. Балада[1], *М. Четібі*[1], *А. Бутрід*[2,3], *А. Бухеджа*[1]

1 – Факультет наук про Землю, кафедра гірничої справи, Університет Баджи Мохтар, м. Аннаба, Алжир, e-mail: fbaladah2@gmail.com
2 – Лабораторія переробки корисних копалин і навколишнього середовища, Університет Баджи Мохтар, м. Аннаба, Алжир
3 – Кафедра цивільного будівництва, Університет імені Аббаса Лагрура, м. Хеншела, Алжир

Мета. Метою проведеного грануло-хімічного й мінералогічного дослідження, реалізованого на бариті двох жил № 4 та 10 родовища Айн Мімуна (Алжир), є ідентифікація руди бариту для визначення можливості вибору надійного методу переробки, що викликано його складною структурою.

Методика. Дослідження проводилося за допомогою рентгенівської дифракції (РД), скануючого електронного мікроскопа (СЕМ), рентгенівської флуоресценції (РФ), аналізу розміру частинок і мікроскопічних спостережень.

Результати. За допомогою дослідницьких приладів було встановлено переважання мінералів бариту, що становлять 51 %, кварцу – приблизно 34 % і кальциту в кількості 9 % з однорідним розподілом у всіх фракціях, за якими спостерігали. Крім того, основними присутніми сполуками (оксидами) є SiO_2, CaO, Fe_2O_3, Al_2O_3, P_2O_5, Na_2O, K_2O, TiO_2 і MnO.

Наукова новизна. Полягає в тому, що вперше був описаний характер розподілу мінералів у жилах № 4 і 10, в яких частинки бариту залягають у кремнеземі, з метою доказу можливості їх переробки.

Практична значимість. Отримані результати підтверджують, з одного боку, що жили № 4 і 10 багаті на барит, а, з іншого боку, те, що можливе виділення частинок бариту з частинок кремнезему. Таким чином, для більш якісного й різноманітного використання руди жил, що аналізуються, ми пропонуємо застосування процесу флотації, так як останній дозволяє отримувати високоякісні концентрати, тому його можна використовувати не тільки в нафтовому секторі, але й у фармацевтичній та інших галузях промисловості .

Ключові слова: *шахта Айн Мімун, баритова руда, жили № 4 і 10, збагачення, Алжир*

The manuscript was submitted 20.09.21.